Three-photon absorption in semiconductor quantum dots: experiment

Xiaobo Feng[1, 2], Yu Long Ang [1], Jun He[1], Cyrus W. J. Beh[3], Hairu Xu[3], Wee Shong Chin[3], and Wei Ji[1,*]

[1]*Department of Physics, National University of Singapore, 2 Science Drive 3, Singapore 117542, Singapore*
[2]*Department of Physics, Wuhan University, Wuhan 430072, China*
[3]*Department of Chemistry, National University of Singapore, 3 Science Drive 3, Singapore 117543, Singapore*
[*]*Corresponding author: phyjiwei@nus.edu.sg*

Abstract: The four-band model, derived under the effective-mass approximation for cubic semiconductor quantum dots (QDs), is compared with experimental measurements on frequency degenerate three-photon absorption (3PA) in CdSe QDs and ZnS QDs. Qualitatively, the model provides the correct prediction on the magnitude of the 3PA cross-sections, which are in the range from 10^{-79} to 10^{-77} $cm^6s^2photon^{-2}$ in the light frequency region of interest. More noticeably, the theoretical conclusion of an increasing tendency in the 3PA cross-sections with increasing dot-size is in agreement with the experiment. The discrepancy is also found for smaller QDs (dot-radius is less than one-third of the exciton Bohr radius), which is attributed to neglecting the mixing among the three valence bands in the theory.

OCIS codes: (190.4180) Multiphoton processes; (190.5970) Semiconductor nonlinear optics including MQD; (320.7110) Ultrafast nonlinear optics.

References and links

1. X. Michalet, F. F. Pinaud, L. A. Bentolila, J. M. Tsay, S. Doose, J. J. Li , G. Sundaresan, A. M. Wu , S. S. Gambhir, and S.Weiss, "Quantum Dots for Live Cells, in Vivo Imaging, and Diagnostics," Science **307,** 538 (2005).
2. D. R. Larson, W. R. Zipfel, R. M. Williams, S. W. Clark, M. P. Bruchez, F. W. Wise, and W. W. Webb, "Water-Soluble Quantum Dots for Multiphoton Fluorescence Imaging in Vivo," Science **300**, 1434 (2003).
3. B. Dubertret, P. Skourides, D. J. Norris, V. Noireaux, A. H. Brivanlou, and A. Libchaber, "In Vivo Imaging of Quantum Dots Encapsulated in Phospholipid Micelles," Science **298**, 1759 (2002).
4. G. S. He, K. T. Yong, Q. D. Zheng, Y. Sahoo, A. Baev, A. I. Ryasnyanskiy, and P. N. Prasad, "Multi-photon excitation properties of CdSe quantum dots solutions and optical limiting behavior in infrared range," Opt. Express **15**, 12818 (2007).
5. F. E. Hernandez, K. D. Belfield, and I. Cohanoschi, "Three-photon absorption enhancement in a symmetrical charge transfer fluorene derivative," Chem. Phys. Lett. **391**, 22 (2004).
6. F. E. Hernandez, K. D. Belfield, I. Cohanoschi, M. Balu and K. J. Schafer, "Three- and Four-Photon Absorption of a Multiphoton absorbing Fluorescent Probe," Appl. Opt. **43**, 5394 (2004).
7. A. V. Fedorov, A. V. Baranov, and K. Inoue, "Two-photon transitions in systems with semiconductor quantum dots," Phys. Rev. B. **54**, 8627 (1996).
8. J. W. M. Chon, M. Gu, C. Bullen, and P. Mulvaney, "Three-photon excited band edge and trap emission of CdS semiconductor nanocrystals," Appl. Phys. Lett. **84**, 4472 (2004).
9. J. He, W. Ji, J. Mi, Y. Zheng, and J. Y. Ying, "Three-photon absorption in water-soluble ZnS nanocrystals," Appl. Phys. Lett. **88**, 181114 (2006).
10. A. D. Lad, P. P. Kiran, G. R. Kumar, and S. Mahamuni, "Three-photon absorption in ZnSe and ZnSe/ZnS quantum dots," Appl. Phys. Lett. **90**, 133113 (2007).
11. I. M. Lifshits and V. V. Slezov, "The kinetics of diffusional decomposition of super-saturated solid solutions," Zh. Eksp. Teor. Fiz **35**, 479 (1958).
12. P. Lawaetz, "Valence-band Parameters in Cubic Semiconductors," Phys. Rev. B **4**, 3460 (1971).
13. D. J. Norris and M. G. Bawendi, "Measurement and assignment of the size-dependent optical spectrum in CdSe quantum dots," Phys. Rev. B **53**, 16338 (1996).

#92423 - $15.00 USD Received 6 Feb 2008; revised 17 Mar 2008; accepted 17 Mar 2008; published 1 May 2008

14. L. A. Padilha, J. Fu, D. J. Hagan, E. W. Van Stryland, C. L. Cesar, L. C. Barbosa, C. H. B. Cruz, D. Buso, and A. Martucci, "Frequency degenerate and nondegenerate two-photon absorption spectra of semiconductor quantum dots," Phys. Rev. B **75**, 075325 (2007).
15. L. A. Padilha, J. Fu, D. J. Hagan, E. W. Van Stryland, C. L. Cesar, L. C. Barbosa, and C. H. B. Cruz, "Two-photon absorption in CdTe quantum dots," Opt. Express **13**, 6460 (2004).
16. Y. Nosaka, "Finite depth spherical well model for excited states of ultrasmall semiconductor particles: an application," J. Phys. Chem. **95**, 5054 (1991).
17. R. Viswanatha, S. Sapra, T. Saha-Dasgupta, and D. D. Sarma, "Electronic structure of and quantum size effect in III-V and II-VI semiconducting nanocrystals using a realistic tight binding approach," Phys. Rev. B **72**, 045333 (2005).
18. N. Kumbhojkar, V. V. Nikesh, A. Kshirsagar, and S. Mahamuni, "Photophysical properties of ZnS nanoclusters," J. Appl. Phys. **88**, 6260 (2000).
19. S. Sapra, A. Prakash, A. Ghangrekar, N. Periasamy, and D. D. Sarma, "Emission Properties of Manganese-Doped ZnS Nanocrystals," J. Phys. Chem. B **109**, 1663 (2005).
20. M. Sheik-Bahae, A. A. Said, T. H. Wei, D. J. Hagan, and E. W. Van Stryland, "Sensitive measurement of optical nonlinearities using a single beam," IEEE J. Quantum Electron. **26**, 760 (1990).
21. R. L. Sutherland, *Handbook of Nonlinear Optics*, with contributions by D. G. McLean and S. Kirkpatrick, Second Edition, (New York, NY: Marcel Dekker, 2003).
22. J. He, Y. L. Qu, H. P. Li, J. Mi, and W. Ji, "Three-photon absorption in ZnO and ZnS crystals," Opt. Express **13**, 9235 (2005).
23. I. M. Catalano, A. Cingolani, and A. Minafra, "Multiphoton impurity luminescence in zinc sulphide," Opt. Commun. **7**, 270 (1973).

1. Introduction

Recently, semiconductor quantum dots (QDs), or nanocrystals (NCs), have received considerable attention due to their potential applications in optical limiting, bio-labels, biosensors and imaging agents [1-4], employing two-photon absorption (2PA) or three-photon absorption (3PA). Compared with 2PA, longer excitation wavelengths may be utilized in 3PA-based applications to provide deeper penetration depths in absorptive media and higher spatial resolution [5, 6]. A better understanding of 3PA in semiconductor QDs should be of direct relevance to 3PA-based applications. By extending Federov's model [7], we have developed a four-band model for the frequency degenerate 3PA of cubic semiconductor QDs or NCs. To validate the model, we present here the comparison between the model and experimental measurements on the frequency degenerate 3PA cross-sections of CdSe QDs and ZnS QDs.

The 3PA in semiconductor QDs was first reported on CdS QDs. With femtosecond pulsed excitation, Chon and his co-workers [8] measured the three-photon-excited band-edge and trap-state emission from CdS QDs in solution, and they concluded that the 3PA cross-sections should be ~ 10^{-79} $cm^6s^2photon^{-2}$. However, there was uncertainty in their measurements since the three-photon-excited photoluminescence efficiency was assumed. The first unambiguous measurement on the 3PA cross-section of ZnS QDs of 1.3-nm radius was made by He, *et al*., [9] who applied both Z-scan and transient transmission techniques with 120-fs laser pulses to determine it to be ~10^{-78} $cm^6s^2photon^{-2}$ at 780 nm. Very recently, 3PA of CdSe QDs in hexane solution of five different dot-sizes was investigated systematically with femtosecond laser pulses [4]. It is also noticed that Lad, *et al*., experimentally studied the 3PA in ZnSe QDs and ZnSe/ZnS core-shell QDs with picosecond laser pulses [10].

In Section 2.1, we compare the four-parabolic-band model with the size-dependent 3PA cross-sections of CdSe QDs measured by He, *et al.* [4]. In Section 2.2, we also make comparison between the model and 3PA cross-section measurements on ZnS QDs by femtosecond Z-scans in the broad spectral range of 600-750 nm. There is no adjustable parameter in the model. It is found that good agreement can be reached for QDs with dot-sizes being less than the exciton Bohr radius a_B. But discrepancy exists for smaller QDs (radii are less than one-third of the exciton Bohr radius a_B), which is attributed to neglecting the mixing of the valence bands in the model.

#92423 - $15.00 USD Received 6 Feb 2008; revised 17 Mar 2008; accepted 17 Mar 2008; published 1 May 2008

2. Experiment

Following Federov's model [7], we have derived the following analytical expression for the frequency degenerate 3PA cross-sections, σ_3, for ZnS and CdSe QDs, with the Lifshits-Slezov size distribution [11].

$$\sigma_3 = \frac{6\pi\hbar^2\omega^3}{\varepsilon_\omega^{3/2}}\left(\frac{8\pi e^2}{3\omega^2 c}\right)^3 (P\hbar)^2 \sum_{j=1}^{3}\left\langle F_{c,h_j}\right\rangle, \tag{1}$$

where

$$\left\langle F_{c,h_j}\right\rangle = \frac{1}{2\Delta_{h_j}} \sum_{\beta_1,\beta_2,\beta_0} (l_2\delta_{l_2,l_0+1} + l_0\delta_{l_2,l_0-1})(l_1\delta_{l_1,l_2+1} + l_2\delta_{l_1,l_2-1})$$
$$\times T^{c,h_j}_{\beta_1,\beta_2,\beta_0}(R^{(h_j)}_{\beta_1;\beta_0}) \frac{\xi^4_{\beta_2}\xi^2_{\beta_0}\xi^2_{\beta_1}}{(\xi^2_{\beta_2}-\xi^2_{\beta_0})^2(\xi^2_{\beta_1}-\xi^2_{\beta_2})^2} \frac{f(R^{(h_j)}_{\beta_1;\beta_0})}{(R^{(h_j)}_{\beta_1;\beta_0})^3} \tag{2}$$

For the definitions of the symbols and nomenclature, the reader is referred to Ref. [7]. It should be emphasized that there is no free parameter in the calculations and discussion presented in the next section. And the material parameters involved are listed in Table 1.

Table 1. Parameters used in the Calculations for the Investigated Materials

	E_g (eV)	Δ_{so} (eV)	m_c (m_0)	m_{hh} (m_0)	m_{lh} (m_0)	m_{so} (m_0)	$a_B(nm)$
ZnS[9,14]	3.8	0.07	0.28	1.76	0.23	0.4	2.2
CdSe[15]	1.84	0.42	0.11	1.14	0.31	0.49	4.9

2.1 3PA Cross-Sections of CdSe Quantum Dots

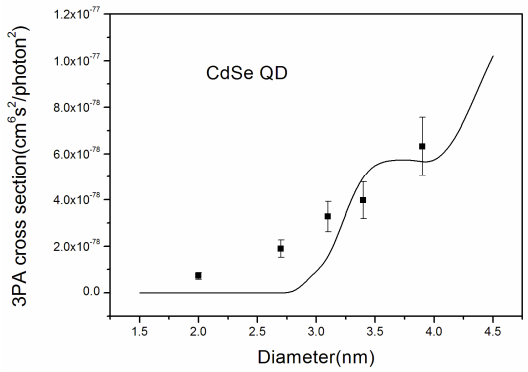

Fig. 1. The 3PA cross-section plotted as a function of the dot diameter for CdSe QDs with the three-photon excitation wavelength of ~1300 nm. The solid line is our theoretical calculation. The solid squares are the data measured by He, *et al.* [4].

The 3PA cross-sections calculated at the wavelength of 1300 nm for CdSe QDs as a function of the average diameter are shown in Fig. 1. It is evident that the overall magnitude of the 3PA cross-section increases with increasing QD diameter, in agreement with the case of two-photon absorption (2PA) [14, 15]. For comparison, we re-plot the experimental results by He, *et al.*, [4] for CdSe QDs with the three-photon excitation wavelength of ~1300 nm. Notice that the 3PA coefficient per QD, σ_3' is defined as $\sigma_3'=\alpha_3/N$ in Ref. [4], where α_3 and N are the 3PA coefficient of the solution and the QD density, respectively. In Fig. 1, we convert it to the 3PA cross-section by the definition of $\sigma_3=(\hbar\omega)^2\alpha_3/N$. As seen from Fig. 1, the theory predicts an

#92423 - $15.00 USD Received 6 Feb 2008; revised 17 Mar 2008; accepted 17 Mar 2008; published 1 May 2008

increasing tendency in the 3PA cross-sections with the increase in the dot-diameter, though it does not increase monotonously. This is consistent with the measurement. Within the experimental errors, a good agreement between the experimental data and the theory can be found, for CdSe QDs of larger diameters ($2R_0$ = ~3.9 and ~3.4 nm). Notice that the exciton Bohr diameter is $2a_B$ = 9.8 nm. Thus, the good agreement can be reached for CdSe QDs with dot's diameter being greater than $2a_B/3$ (= 3.3 nm).

For smaller diameters (less than $2a_B/3$ = 3.3 nm), however, the discrepancy exists, similar to the finding for 2PA in QDs [14, 15]. It was revealed by Padilha, *et al.*, [15] that the mixing of the three valence bands is of importance to smaller QDs. If such mixings are considered and included in a $\vec{k} \cdot \vec{P}$ model, an excellent agreement can be reached for the 2PA in smaller QDs. Similarly, we anticipate the mixing should also play an important role in the 3PA of smaller QDs. And the calculation based on the $\vec{k} \cdot \vec{P}$ model is under way.

2.2 3PA Cross-Sections of ZnS Quantum Dots

To investigate the 3PA cross-sections of ZnS QDs, we freshly prepared the QDs with method described in the following. Precursor of ZnS QDs was prepared by reacting thiobenzoic acid with sodium carbonate and zinc nitrate. Thioglycolic acid (20X capping agent) of 420mL was added to 5mL water. The pH value was adjusted to approximately 11~12 by addition of base (~5mL 2M potassium hydroxide or sodium hydroxide). 0.103g precursor was then dissolved in the reaction mixture, and heated to 100 ^{o}C after degassing and filling the reaction set-up with nitrogen gas. After 30 minutes the reaction was stopped by placing the reaction mixture into an ice bath. The pH value was readjusted back to around 7 by addition of acid so as to reduce the QD solubility in water, thereby increasing the ease of precipitation. The reaction mixture was then left to stand for 7 days to allow the aggregation of smaller crystals into larger ones. 2-propanol was then added until turbidity was observed and the mixture was centrifuged. The precipitate was washed with 2-propanol and dried under vacuum. The pellet of the QDs was vacuum-dried at room temperature overnight, and the final product in the powder form could be re-dissolved in water.

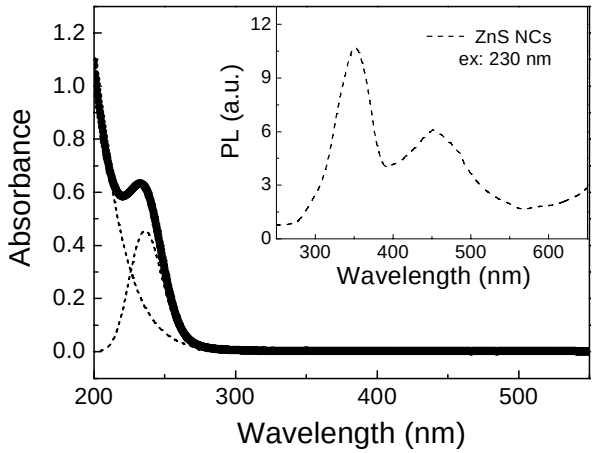

Fig. 2. UV-VIS one-photon absorption (thick solid line:—) spectrum, together with the Gaussian fitting bands (dotted lines:···), of the ZnS QDs. The inset shows the PL (dashed line:---) spectrum excited at 230 nm.

With a UV-visible spectrophotometer (Shimadzu, UV-1700), the one-photon absorption spectrum of the thioglycol-capped ZnS QDs in aqueous solution was recorded and is shown in Fig. 2. Both sharp optical absorption edge and well-defined excitonic feature are indicative of a narrow size distribution of the QDs. The 1.3-nm size of the ZnS QDs was estimated by the

#92423 - $15.00 USD Received 6 Feb 2008; revised 17 Mar 2008; accepted 17 Mar 2008; published 1 May 2008

calculation based on effective mass approximation [16] and realistic tight binding calculation [17]. Broadening of the excitonic transition is primarily due to the inhomogeneity arising from size dispersion. A size distribution of ~ 8% can be estimated with the 520-meV width of the excitonic transition of $1S(e)$–$1S_{3/2}(h)$ observed in Fig. 2. The inset of Fig. 2 displays two PL emission bands (peaked at 350 and 450 nm), recorded by a Jasco FP-6300 spectrofluorometer for the ZnS QDs. The PL emission peak at 350 nm, which is red-shifted compared to the excitonic transition (~ 232 nm), is consistent with the observation by Kumbhojkar, *et al.*, [18] and Sapra, *et al*., [19] for un-doped ZnS QDs. The change of excitation wavelength only led to the alteration in the intensity of the emission peaks. The strong emission bands could be attributed to the carrier recombination of the sulfur defect states, which are mostly on the surface of the QDs [16, 19].

The room-temperature 3PA of the ZnS QDs in aqueous solution was investigated with a standard Z-scan technique [20]. The 1-mJ, 1-kHz, 120-fs laser pulses were generated by a Ti:Sapphire regenerative amplifier (Quantronix, Titan), which was seeded by an erbium-doped fiber laser (Quantronix, IMRA). The wavelengths were tunable as the laser pulses passed through an optical parametric amplifier (Quantronix, TOPAS). The spatial distribution of the pulses was nearly Gaussian, after passing through a spatial filter. The high quality of the Gaussian beam was confirmed by the M^2-factor measurement, showing that the value of M^2 was close to the unity. The laser beam was divided by a beam splitter into two parts. The reflected part was taken as the reference representing the incident laser power and the transmitted beam was focused with a lens (f = 25 cm) onto the ZnS aqueous solution which was placed in a 10-mm-thick quartz cell. Two light power probes (Laser Probe, RkP-465 HD) were used to record both the incident and transmitted laser power simultaneously. A computer-controlled translation stage was employed to move the cell along the propagation direction (Z-axis) of the laser pulses. For the open-aperture (OA) Z-scans, extreme care was taken to ensure the entire collection of the transmitted light, and thus, self-lensing effects were eliminated.

It should be pointed out that the ZnS QDs possessed the high photostability in aqueous solution with high-power laser pulses because their one-photon absorption and PL spectra were measured before and after the pulsed laser irradiation; no measurable difference was observed. For calibration, similar 3PA measurements were conducted on a 0.5-mm-thick cubic ZnS bulk crystal (Semiconductor Wafer, Inc.) with laser polarization perpendicular to its <111> axis. All the Z-scans reported here were performed with excitation irradiances below the damage threshold.

Figure 3 illustrates the typical OA Z-scan curves for both the ZnS QD solution and the ZnS bulk crystal, where excitation irradiance I_{00} is denoted as the peak, on-axis irradiance at the focal point (z = 0) within the sample. I_{00} is related to the incident irradiance by taking Fresnel's surface reflection into consideration. By taking into account of spatial and temporal Gaussian pulses, the normalized energy transmittance, $T_{OA}(z)$, is given by [21,22].

$$T_{OA} = \frac{1}{\sqrt{\pi}\, p_0} \int_{-\infty}^{\infty} \ln\left[\sqrt{1 + {p_0}^2 \exp\left(-2x^2\right)} + p_0 \exp\left(-x^2\right)\right] dx \qquad (3)$$

where $p_0 = \sqrt{2\alpha_3 I_0^2 L'_{eff}}$, $I_0 = I_{00}/(1+z^2/z_0^2)$ is the excitation intensity at position z, $z_0 = \pi w_0^2/\lambda$ is the Rayleigh range, w_0 is the minimum beam waist, λ is the laser free-space wavelength, $L'_{eff} = \frac{1-\exp(-2\alpha_0 L)}{2\alpha_0}$ is the effective sample length, α_0 is the linear absorption coefficient, and L is the sample length. The 3PA coefficient α_3 can be extracted by fitting Eq. (3) to the OA Z-scan curves. Finally, the 3PA cross-section (σ_3) can be inferred from

#92423 - $15.00 USD Received 6 Feb 2008; revised 17 Mar 2008; accepted 17 Mar 2008; published 1 May 2008

$\sigma_3=(\hbar\omega)^2\alpha_3/N$. Note that the large experimental errors result primarily from the uncertainty in determining the density of the ZnS QDs in solution.

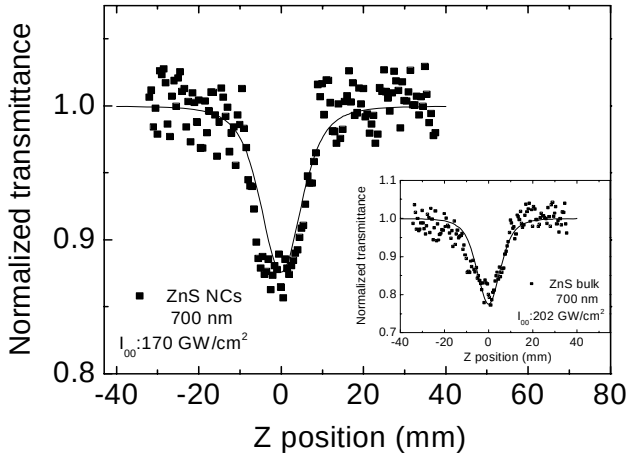

Fig. 3. Typical open-aperture Z-scans at 700 nm for the ZnS QDs. The symbols denote the experimental data while the solid lines are theoretically fitted curves employing the Z-scan theory described in the text. The inset shows the Z-scan curves for the ZnS bulk crystal.

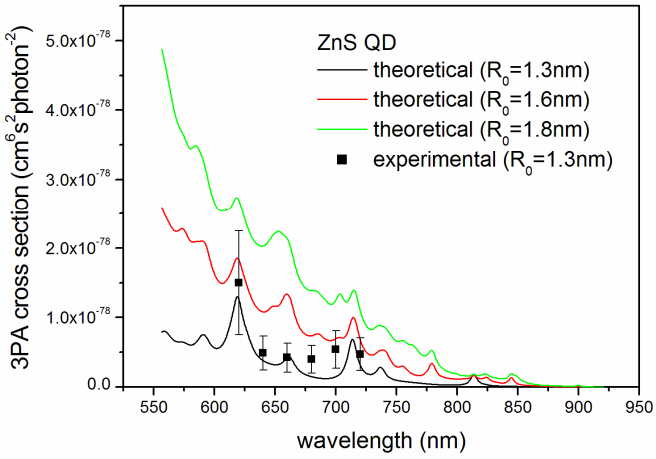

Fig. 4. 3PA cross-sections calculated as a function of the wavelength for ZnS QDs. The solid squares are the experimental data.

The measured 3PA cross-section spectrum for the 1.3 nm-sized water-soluble ZnS QDs is shown in Fig. 4. For comparison, the theoretical calculations are also presented. Obviously, a good agreement is found between the theory and the experiment within the experimental errors. The magnitude of the 3PA cross-sections that we calculated and measured is at least one order larger than those of ZnS bulk crystal [23].This enhancement can be attributed to the quantum confinement effect since ZnS QDs' average radius ($R_0 \sim$ 1.3 nm) is smaller than the Bohr exciton radius (a_B = 2.2 nm). The good agreement demonstrates again that our model explains the data well for QD sizes in the range from being smaller than the exciton Bohr radius, a_B to being greater than $a_B/3$.

#92423 - $15.00 USD Received 6 Feb 2008; revised 17 Mar 2008; accepted 17 Mar 2008; published 1 May 2008

3. Conclusion

The four-band model, that is derived under the effective-mass approximation for semiconductor QDs of O_h -symmetry, is compared with experimental measurements on the frequency degenerate 3PA cross-sections of CdSe QDs and ZnS QDs. Qualitatively, the model provides the correct prediction on the magnitude of the 3PA cross-sections, which are in the range from 10^{-79} to 10^{-77} $cm^6s^2photon^{-2}$ in the light frequency region of interest. More noticeably, the theoretical conclusion of an increasing tendency in the 3PA cross-section spectra with the increase of dot-size is in agreement with the experiment. The discrepancy is also found for smaller QDs (dot-radius is less than the one-third of the exciton Bohr radius), which is attributed to neglecting the mixing among the three valence bands in the theory.

Acknowledgment

Xiaobo Feng gratefully acknowledges the scholarship from the China Scholarship Council. We also thank the financial support of the National University of Singapore (R-144-000-213-112).

#92423 - $15.00 USD Received 6 Feb 2008; revised 17 Mar 2008; accepted 17 Mar 2008; published 1 May 2008